

Optical dephasing by nonequilibrium phonons in  $\text{LaF}_3$ 

R. S. Meltzer

IBM Research Laboratory, San Jose, California 95193  
and Department of Physics and Astronomy, University of Georgia, Athens, Georgia 30602

R. M. Macfarlane

IBM Research Laboratory, San Jose, California 95193

(Received 26 December 1984)

Phonon-induced coherence loss (PICL) is produced by a monoenergetic nonequilibrium distribution of phonons in  $\text{LaF}_3:\text{Pr}^{3+}$ . The phonons are generated by relaxation between excited states of the  $\text{Pr}^{3+}$  ion after selective excitation with a pulsed, tunable dye laser. The optical dephasing is observed from the effect on the free-induction decay of  $\text{Pr}^{3+}$  ions whose excited-state level separation is resonant with the phonons. It is shown that PICL is a sensitive detector of monoenergetic phonons, and can be used to study phonon dynamics. The observed rate of optical dephasing is reduced relative to an equivalent occupation of  $23\text{-cm}^{-1}$  phonons produced thermally.

## I. INTRODUCTION

Phonon-induced processes are the major source of dephasing in insulating solids at all but the lowest of temperatures. In the optical regime these processes are usually identified by the temperature dependence of either optical linewidths (frequency domain) or the decay of coherent transient signals (time domain). In these cases a broad thermal distribution of phonons is present. The particular phonon-induced dephasing mechanism is obtained from the specific nature of the temperature dependence. Mechanisms of importance include the direct process involving one-phonon absorption to nearby excited states which gives rise to an exponential dependence of dephasing on temperature, and Raman processes which produce a  $T^7$  behavior.<sup>1</sup> Usually several mechanisms appear simultaneously, at least over some range of temperature. In addition, there are often many electronic states whose energies relative to that of the ground or excited state involved in the optical transition fall within the phonon spectrum. When this is the case, phonons at all these resonant energies contribute to the dephasing, making it difficult, and often impossible, to isolate the individual contributions.

We report the first observation of optical dephasing produced by a monoenergetic nonequilibrium distribution of phonons. We call this effect phonon-induced coherence loss (PICL). The system studied is  $\text{LaF}_3$  containing 0.05 at. %  $\text{Pr}^{3+}$ . Optical free-induction decay (FID) is observed<sup>2</sup> on the  ${}^3H_4(\text{I}) \rightarrow {}^1D_2(\text{I})$  transition of the  $\text{Pr}^{3+}$  ion at  $5925 \text{ \AA}$ . The nonequilibrium phonons are resonant with the  ${}^1D_2(\text{I}) \rightarrow {}^1D_2(\text{II})$  transition. These resonant  $23\text{-cm}^{-1}$  phonons are absorbed by the excited  $\text{Pr}^{3+}$  ions causing dephasing. The experiments described in this paper have an impact on two distinct areas.

The first area of impact relates to the isolation and detailed study of specific relaxation pathways by the introduction of coherence loss with monoenergetic phonons. In previous work,<sup>3-6</sup> phonon-induced relaxation in the

${}^3H_4$  and  ${}^1D_2$  states of  $\text{LaF}_3:\text{Pr}^{3+}$  under conditions of thermal equilibrium has been investigated extensively. In this case a broad distribution of phonons is present. The temperature dependence of relaxation processes in the ground manifold above 80 K was first studied by Yen *et al.*<sup>3</sup> using  ${}^3P_0$  absorption line shapes. They identified the direct process as the major dephasing mechanism but could not separate the contribution from the 57- and 76- $\text{cm}^{-1}$  ground-state levels. Erickson<sup>4</sup> extended these measurements down to 10 K for both the ground and  ${}^1D_2$ -excited states using fluorescence line narrowing and identified dephasing due to the direct process with the first excited  ${}^1D_2$  state at  $23 \text{ cm}^{-1}$  (see Fig. 1). Erickson obtained a value of  $T_1(\text{II}) = 225 \text{ ps}$  for the population decay time of the  ${}^1D_2(\text{II})$  state. Macfarlane *et al.*<sup>5</sup> confirmed these results at very low temperatures ( $< 5 \text{ K}$ ) from the temperature dependence of the optical free-induction decay. Kohmoto *et al.*<sup>6</sup> examined the dephasing as a function of temperature with photon echoes on the  ${}^3H_4(\text{I}) \rightarrow {}^1D_2(\text{I})$  transition and were able to isolate the contribution to the dephasing of the direct process involving excited com-

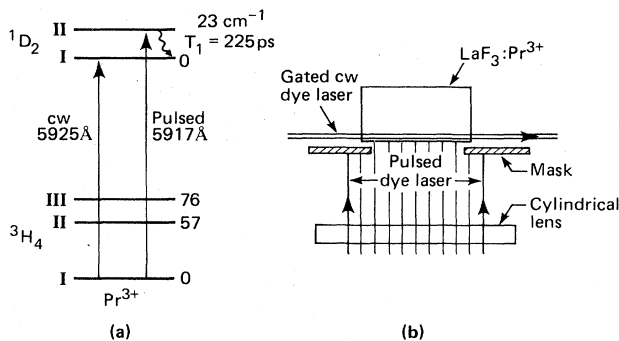


FIG. 1. (a) Energy-level diagram of  $\text{Pr}^{3+}$  in  $\text{LaF}_3$  showing the low-lying crystal-field levels in  ${}^3H_4$  and  ${}^1D_2$ . (b) Experimental geometry for PICL experiments.

ponents of the ground state at 57 and 76  $\text{cm}^{-1}$ . In the results described in the present work, dephasing is produced solely from the monoenergetically prepared 23- $\text{cm}^{-1}$  phonons. It is observed that the rate of coherence loss due to the direct process connecting  $^1D_2(\text{I})$  and  $^1D_2(\text{II})$  is different from that which occurs in the presence of a broad distribution of thermal phonons.

The second area of impact concerns the use of PICL as a new frequency-selective detector to study the dynamics of high-frequency phonons. Several other techniques have been used to study the dynamics of nonequilibrium phonons in  $\text{LaF}_3$ . Godfrey *et al.*<sup>7</sup> used hot luminescence from  $^1D_2(\text{II})$  after pulsed-laser generation of monoenergetic phonons. They found a lifetime of 210 ns for the 23- $\text{cm}^{-1}$  phonons in a  $\text{LaF}_3:0.05$  at. %  $\text{Pr}^{3+}$  sample. Will *et al.*<sup>8</sup> utilized heat-pulse phonon generation and hot-luminescence detection from the upper Zeeman level of the  $^4S_{3/2}(\text{I})$  state of  $\text{Er}^{3+}$  split in a magnetic field. A lifetime of 1  $\mu\text{s}$  was obtained at 23  $\text{cm}^{-1}$ , and an  $\omega^5$  frequency dependence was observed in the frequency range 22–37  $\text{cm}^{-1}$ . In the  $\text{LaF}_3:0.05$  at. %  $\text{Pr}^{3+}$  sample used in the present experiments, we find a 23- $\text{cm}^{-1}$ -phonon lifetime of 500 ns. The different values of the 23- $\text{cm}^{-1}$ -phonon lifetime indicate that their lifetimes are somewhat sample dependent. Vibronic sideband spectroscopy has also been used<sup>9</sup> in a double-doped sample of  $\text{LaF}_3$  containing 0.05 at. %  $\text{Pr}^{3+}$  and 0.3 at. %  $\text{Er}^{3+}$ . The lifetimes of 41- $\text{cm}^{-1}$  and 54- $\text{cm}^{-1}$  phonons were found to be 40 and 5 ns, respectively. Schosser and Dlott<sup>10</sup> obtained a lifetime of 0.38 ns for 78- $\text{cm}^{-1}$  optical phonons in  $\text{LaF}_3:2$  at. %  $\text{Ce}^{3+}$  using picosecond coherent anti-Stokes Raman spectroscopy. We show here that PICL is a highly sensitive detector for nonequilibrium phonons, providing both good temporal and spectral resolution, and that it can be used to obtain the lifetime of resonant phonons.

## II. EXPERIMENTS

Phonons are generated by selectively pumping the  $^3H_4(\text{I}) \rightarrow ^1D_2(\text{II})$  transition at 5917 Å with a Nd:YAG-pumped tunable dye laser (where YAG is yttrium aluminum garnet) whose bandwidth was 2 GHz. Rapid relaxation [ $T_1(\text{II})=225$  ps] to  $^1D_2(\text{I})$  generates a monoenergetic distribution of phonons which are resonant with the  $^1D_2(\text{I}) \rightarrow ^1D_2(\text{II})$  transition (see Fig. 1). The FID was observed on the  $^3H_4(\text{I}) \rightarrow ^1D_2(\text{I})$  transition, excited by an actively stabilized cw tunable dye laser whose frequency was switched by an intracavity electrooptic phase modulator.<sup>11</sup> The 20-mW, 1-MHz-bandwidth laser output was gated on to the sample for 20  $\mu\text{s}$  with an acoustooptic modulator.<sup>5</sup> After a 10- $\mu\text{s}$  preparation time, the laser frequency was shifted by 20 MHz. After 5  $\mu\text{s}$  the laser was returned to the original frequency. The frequency-shifted laser acts as a local oscillator for the heterodyne detection of the FID. The heterodyne signal was detected with an avalanche photodiode after filtering with a monochromator to reject the scattered laser light at the 5917-Å phonon-generator wavelength.

The experimental geometry is shown in Fig. 1(b). The cw dye laser was focused to a 50- $\mu\text{m}$  spot in the sample. The Nd:YAG-pumped dye laser output propagated at a

right angle to the cw beam and was focused with a cylindrical lens to a line 100  $\mu\text{m}$  thick and 10 mm long which overlapped the cw beam. Because of the strong absorption of the pulsed dye laser on the  $^1D_2(\text{II})$  level ( $\alpha \approx 10$   $\text{cm}^{-1}$ ), the cw laser beam is brought close to the surface through which the pulsed laser enters the sample. The timing sequence and delay between the frequency switch of the cw dye laser and the output of the pulsed dye laser was continuously variable electronically.

## III. EXPERIMENTAL RESULTS

The FID signal in the absence of the 23- $\text{cm}^{-1}$  phonons is shown in Fig. 2, top trace. It exhibits a decay time of 1.5  $\mu\text{s}$ , corresponding to a dephasing time of 3  $\mu\text{s}$ . This is somewhat shorter than the true low-temperature dephasing time of 5  $\mu\text{s}$  obtained from photon-echo experiments,<sup>12</sup> due to laser-frequency jitter during the preparation time. When phonons are generated during the FID decay, an enhancement of the dephasing rate occurs (Fig. 2). With an energy input of 300  $\mu\text{J}$  (not shown), the coherence decays in less than one cycle of the 20-MHz FID signal. There is a small remaining FID signal which arises from the 0.5-mm end sections of the sample which are masked so as to prevent surface heating of the end faces by the pulsed laser. The heating produces bubbles in the superfluid helium introducing strong oscillatory signals which interfere with the measurement of the FID. As the phonon-generating laser energy is reduced, the FID signal decays over many cycles but at a rate which is still faster than that observed under 1.2-K equilibrium conditions. No instantaneous change in the amplitude was observed as a consequence of the optical excitation by the pulsed dye laser, indicating the absence of contributions to the coherence decay from population changes.

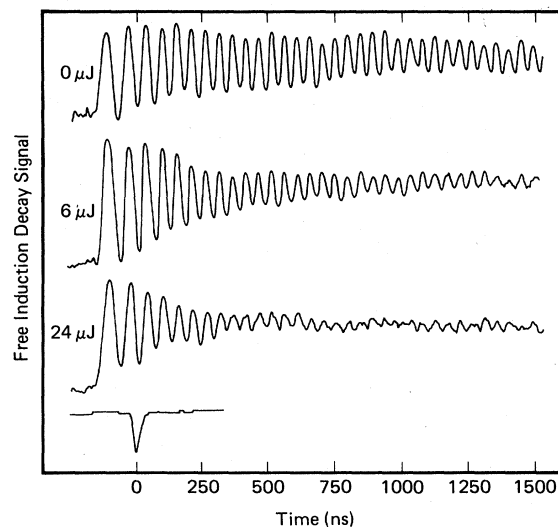


FIG. 2. Free-induction-decay signals as a function of the energy of the pulsed tunable dye laser used in a side-pumping geometry. The FID occurs on the  $^3H_4(\text{I}) \rightarrow ^1D_2(\text{I})$  transition and the pulsed dye laser, whose temporal location is shown in the bottom trace, is tuned to the  $^3H_4(\text{I}) \rightarrow ^1D_2(\text{II})$  transition.

The amplitude of the FID signal is plotted as a function of time in Fig. 3 for several pulsed-laser energies. The background signal due to the masked end faces has been subtracted. In addition, the data have been corrected for the equilibrium contribution to the dephasing so that they represent only the contribution from the nonequilibrium phonons. These data are an average of three to five decay measurements.

For the higher pulse energies where the FID decays in a time short compared to the  $23\text{-cm}^{-1}$ -phonon lifetime ( $T_{\text{ph}}=500\text{ ns}$  in this sample) the decay is exponential. However, for the lower pulse energies the decay is highly nonexponential due to the finite lifetime of the  $23\text{-cm}^{-1}$  resonant phonons whose contribution to the dephasing rate decreases with time as they decay into nonresonant phonons. It is under this lower pulse energy condition that PICL contains information on the phonon lifetime.

When the pulsed laser is tuned to the  ${}^1D_2(\text{I})$  transition the dephasing rate is only slightly enhanced, even under maximum laser energy, due to heat produced by surface heating, cross-relaxation, up-conversion or other nonradiative relaxation process, but the effect is always at least two orders of magnitude less than that of the resonant phonons created by pumping  ${}^1D_2(\text{II})$ .

Phonons were also generated at times  $\Delta t$  prior to the FID signal. For strong pulsed excitation and times  $\Delta t \leq 1\ \mu\text{s}$  only the FID signal from the masked ends is observed. However, even for much weaker pulsed-laser excitation conditions and for  $\Delta t \gg T_{\text{ph}}$ , significant dephasing effects

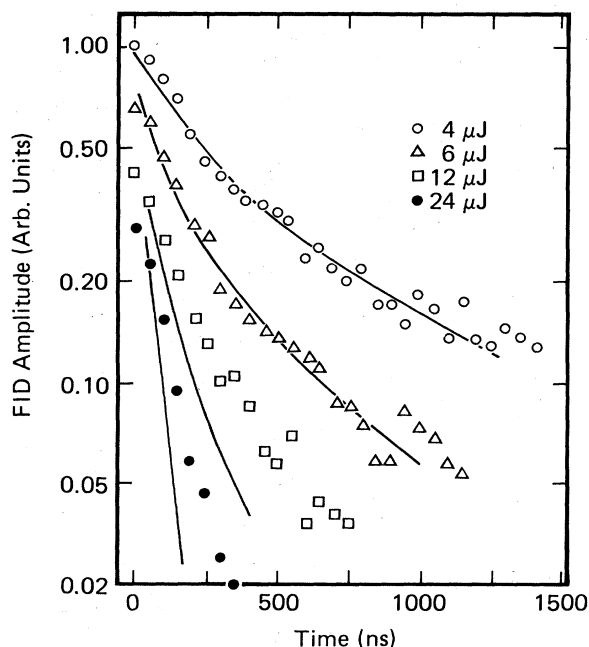


FIG. 3. Time dependence of the FID amplitude,  $23\text{-cm}^{-1}$ -phonon contribution only, for several pulsed-laser energies. The data have been corrected for end effects. The curves are fits to the  $4\text{-}\mu\text{J}$  data according to Eq. (4) for several values of  $T_{\text{ph}}$  with an initial  $23\text{-cm}^{-1}$ -phonon occupation number  $\bar{n}_{23}(0)=3.0 \times 10^{-4}$  chosen to give the observed initial slope.

are evident. For example, the nonequilibrium phonon contribution to the dephasing as a function of  $\Delta t$  is shown by the circles in Fig. 4 for  $24\text{-}\mu\text{J}$  pulsed-laser energies. It is clear that significant dephasing effects persist for at least  $100\ \mu\text{s}$ .

In analyzing the FID signals it is necessary to know the time dependence of the occupation numbers of the  $23\text{-cm}^{-1}$  phonons which produce the dephasing. This can be obtained from the time dependence of the ratio of the  ${}^1D_2(\text{II})$  to the  ${}^1D_2(\text{I})$  fluorescence intensity after correcting for their relative oscillator strengths. This technique has been used successfully to obtain phonon lifetimes in this and other materials.<sup>7,8</sup> The case of  $300\text{-}\mu\text{J}$  pulsed-laser energy is shown in Fig. 5. The initial decay rate (see inset) gives a  $23\text{-cm}^{-1}$  phonon lifetime of  $500\text{ ns}$ . As noted previously,<sup>7</sup> a long tail on the  ${}^1D_2(\text{II})$  to  ${}^1D_2(\text{I})$  fluorescence intensity ratio persists out to  $1\text{ ms}$ . This signifies the presence of  $23\text{-cm}^{-1}$  phonons whose occupation numbers are in excess of those indicated by the bath temperature, even at times much greater than the phonon lifetime, in agreement with the optical dephasing results.

The  $23\text{-cm}^{-1}$  phonon occupation and its resulting effects on the optical dephasing can be understood in terms of three time regimes. For times of the order of the phonon lifetime ( $T_{\text{ph}}=500\text{ ns}$ ) the phonon energy is mainly monoenergetic at  $23\text{ cm}^{-1}$ . At intermediate times the decay products of the  $23\text{-cm}^{-1}$  phonons are trapped in the excited volume due to elastic scattering from the  $\text{Pr}^{3+}$  impurity ions. Under these conditions they may recombine, maintaining the  $23\text{-cm}^{-1}$ -phonon population above that expected at the  $1.2\text{-K}$  bath temperatures for times much greater than the  $23\text{-cm}^{-1}$ -phonon lifetime. At later times the thermal energy can diffuse out of the excited volume into the whole sample, raising the crystal temperature somewhat above that of the bath. Finally after  $1\text{ ms}$ , the sample returns to the bath temperature.

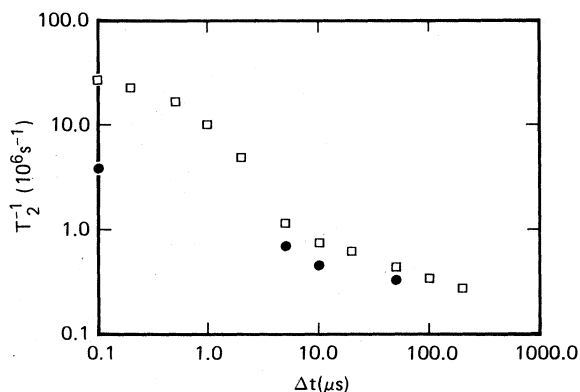


FIG. 4.  $23\text{-cm}^{-1}$ -phonon contribution to the dephasing rate of the  ${}^3H_4(\text{I}) \rightarrow {}^1D_2(\text{I})$  transition for  $24\text{-}\mu\text{J}$  pulsed-laser energy. Circles are data obtained from the FID data, squares are dephasing rates predicted from Eq. (1) and  $\bar{n}_{23}(t)$  obtained from the time dependence of the ratio of the  ${}^1D_2(\text{II})$  to the  ${}^1D_2(\text{I})$  luminescence intensity.

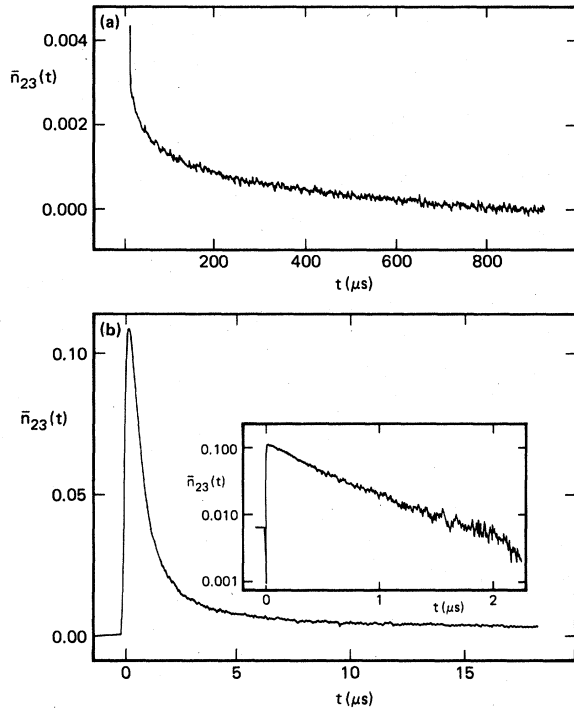


FIG. 5. Time dependence of  $\bar{n}_{23}(t)$ , obtained from the  ${}^1D_2(\text{II})$  to  ${}^1D_2(\text{I})$  luminescence intensity ratio for 300- $\mu\text{J}$  pulsed energy. Note the same data are shown on different time scales. The inset shows a logarithmic plot.

#### IV. COMPARISON OF DEPHASING WITH HOT LUMINESCENCE

The dephasing of the FID signal results from the absorption of the resonant 23-cm<sup>-1</sup> phonons. Therefore, the nonequilibrium phonon contribution to the dephasing rate,  $T_2^{-1}$ , can be related directly to the population relaxation time of  ${}^1D_2(\text{II})$  [ $T_1(\text{II})=225$  ps] and the occupation number of resonant 23-cm<sup>-1</sup> phonons  $\bar{n}_{23}(t)$ ,

$$T_2^{-1}(t) = T_1^{-1}(\text{II})\bar{n}_{23}(t). \quad (1)$$

We first consider the case of constant pulsed-laser energy at varying times  $\Delta t$  prior to the initiation of the FID signal. For time  $\Delta t \gg T_{\text{ph}}$ , we expect the occupation number of 23-cm<sup>-1</sup> phonons to vary slowly compared to the decay time of the FID signal. The decay rate of the FID signal is calculated from the experimentally obtained graphs of  $\bar{n}_{23}(t)$  such as Fig. 5. These calculated decay rates are plotted (squares) in Fig. 4 along with the observed FID decay rates at these same values of  $\Delta t$  (circles). For  $\Delta t > 5 \mu\text{s}$  the agreement is very good. However, for times  $\Delta t > 1 \mu\text{s}$  the dephasing rate is about a factor of 6 less than that calculated from the occupation number.

The probable explanation for this anomalously slow dephasing rate at early times lies in the fact that only a narrow distribution of resonant phonons is present. The calculated dephasing rate assumes a thermal distribution of phonons, a distribution which extends well out into the wings of the resonance. However, the initial distribution of phonons is prepared by pumping the  ${}^1D_2(\text{II})$  state with

a laser whose spectral width (2 GHz) is much less than the  ${}^3H_4(\text{I}) \rightarrow {}^1D_2(\text{II})$  inhomogeneous linewidth (6 GHz). It can be expected that the spectral distribution of phonons generated in the relaxation to  ${}^1D_2(\text{I})$  will be narrowed compared to the full  ${}^1D_2(\text{II}) \rightarrow {}^1D_2(\text{I})$  inhomogeneous resonance width, but broad relative to the homogeneous width (0.7 GHz). As a result, all of the phonons generated by the pulsed laser in the optical dephasing experiments will not be resonant with the ions prepared coherently with the cw laser (bandwidth  $\approx 1$  MHz). On the other hand, the phonon occupation numbers measured in the relative-luminescence-intensity experiments are obtained by generating phonons which are of necessity resonant with the luminescent ions since one laser prepares both the phonons and the excited ions. Thus the ions undergoing dephasing see an effective resonant-phonon occupation number which is reduced relative to that obtained from luminescence.

We next consider the case of phonon generation during the FID signal. For the case of large resonant-phonon occupation number [ $\bar{n}_{23}(0) > 10^{-2}$ ], the dephasing occurs in a time short compared to  $T_{\text{ph}}$  and  $\bar{n}_{23}(t)$  can be constant during the dephasing. However, for smaller  $\bar{n}_{23}(0)$ , the resonant phonons decay during the dephasing and, as a result, the FID decay is nonexponential. The instantaneous dephasing rate,  $T_2^{-1}(t)$  is related to  $\bar{n}_{23}(t)$  through Eq. (1).

We define a fractional FID amplitude,  $f(t)$ , which is the amplitude at time  $t$  divided by the amplitude immediately before phonon generation.  $f(t)$  decays according to the rate equation

$$\frac{df(t)}{dt} = -2[T_1^{-1}(\text{II})\bar{n}_{23}(t) + (T_2')^{-1}]f(t), \quad (2)$$

where  $T_2'$  is the dephasing time in the absence of phonon injection. The solution to Eq. (2) is

$$\ln[f(t)] = -2\bar{n}_{23}(0)T_1^{-1}(\text{II}) \int_0^t [\bar{n}_{23}(t)/\bar{n}_{23}(0)] dt - 2(T_2')^{-1}t. \quad (3)$$

$\bar{n}_{23}(t)$  can be obtained experimentally from the time dependence of the ratio of the  ${}^1D_2(\text{II})$  to the  ${}^1D_2(\text{I})$  luminescence. If  $\bar{n}_{23}(t)$  decays exponentially, as appears to be the case for  $t \leq 2 \mu\text{s}$  (see inset, Fig. 5), then

$$\ln[f(t)] = -2\bar{n}_{23}(0)T_1^{-1}(\text{II})T_{\text{ph}}(1 - e^{-t/T_{\text{ph}}}) - 2(T_2')^{-1}t. \quad (4)$$

The experimentally observed  $f(t)$  is plotted in Fig. 3 along with the values calculated from Eq. (4) for several values of  $T_{\text{ph}}$ . The value of  $\bar{n}_{23}$  at  $t=0$  is obtained from the initial slope of the decay. For the 4- $\mu\text{J}$  pulsed-laser energy data it is found to be  $\frac{1}{6}$  that obtained from the luminescence ratio data as noted previously. We see that the nonexponential behavior of  $f(t)$  is well described with a phonon lifetime  $T_{\text{ph}} = 500$  ns, in agreement with the hot luminescence data. It should therefore be possible to use  $f(t)$  to obtain  $T_{\text{ph}}$  in cases where it is not possible to observe the hot luminescence. This can occur either when  $\bar{n}_{23}(t)$  is very small or the luminescence is masked by background luminescence. In general hot luminescence is

the preferred method since with the use of PICL, phonon occupation numbers are obtained from the time derivative of the coherence decay rather than directly from the luminescence.

### V. CONCLUSIONS

PICL is a new tool with which to investigate both electron-phonon interactions and phonon dynamics. Through the use of a monoenergetic distribution of non-thermal phonons at low temperatures, specific relaxation processes can be made to dominate. In this paper the relaxation channel which is enhanced, namely the direct process connecting the  $^1D_2(\text{I})$  and  $^1D_2(\text{II})$  levels of  $\text{Pr}^{3+}$ , is the same one which dominates in the low-temperature regime at thermal equilibrium, but this is not an inherent limitation of PICL. The effect of monochromatic phonons whose frequency distribution is narrower than the inhomogeneous resonance width is found to be reduced relative to that of a thermal distribution of phonons of equivalent occupation number at the resonant frequency.

With PICL it is possible to observe the presence of nonequilibrium phonons of a particular frequency with great sensitivity. In the present case occupation numbers of  $10^{-4}$  can be detected, but in some systems, detection

levels as low as  $10^{-7}$  are to be expected. Parameters which lead to these sensitivities are short population relaxation times of upper electronic states, e.g.,  $T_1(\text{II})$ , and long coherence times,  $T_2$ . In addition, PICL has good spectral, spatial, and temporal resolution. Spectral resolution is limited to excited-state inhomogeneous resonance widths, typically 1–10 GHz. Temporal resolution using FID techniques is determined by the heterodyne frequency. Although this was only 20 MHz in our experiments, much larger frequencies are possible, limited ultimately by detector frequency response and the extent of the laser frequency shift. Although these experiments were conducted using FID techniques, we point out that PICL can be utilized with any coherent transient measurement. We have, for instance, observed PICL with  $\text{Pr}^{3+}$  ions in  $\text{YAlO}_3$  using photon echoes generated by gated cw laser.

### ACKNOWLEDGMENTS

One of us (R.S.M.) would like to thank IBM for its hospitality during the course of this work and the U.S. Army Research Office for its partial support of this project. We express our appreciation to R. M. Shelby for many helpful suggestions.

- 
- <sup>1</sup>D. E. McCumber and M. D. Sturge, *J. Appl. Phys.* **34**, 1682 (1963).  
<sup>2</sup>A. Z. Genack, R. M. Macfarlane, and R. G. Brewer, *Phys. Rev. Lett.* **37**, 1078 (1976).  
<sup>3</sup>W. M. Yen, W. C. Scott, and A. L. Schawlow, *Phys. Rev.* **136**, A271 (1964).  
<sup>4</sup>L. E. Erickson, *Opt. Commun.* **15**, 246 (1975).  
<sup>5</sup>R. M. Macfarlane, A. Z. Genack, S. Kano, and R. G. Brewer, *J. Lumin.* **18/19**, 933 (1979).  
<sup>6</sup>T. Kohmoto, H. Nakatsuka, and M. Matsuoka *Jpn. J. Appl. Phys.* **22**, L571 (1983).  
<sup>7</sup>L. Godfrey, J. E. Rives, and R. S. Meltzer, *J. Lumin.* **18/19**, 929 (1979).  
<sup>8</sup>J. M. Will, W. Eisfeld, K. F. Renk, and S. Haussühl, *Appl. Phys.* **A31**, 191 (1983).  
<sup>9</sup>R. S. Meltzer, J. E. Rives, and G. S. Dixon, *Phys. Rev. B* **28**, 4786 (1983).  
<sup>10</sup>C. L. Schosser and D. D. Dlott, *Phys. Rev. B* **30**, 2149 (1984).  
<sup>11</sup>R. G. Brewer and A. Z. Genack, *Phys. Rev. Lett.* **36**, 959 (1976).  
<sup>12</sup>R. M. Macfarlane, R. M. Shelby, and R. L. Shoemaker, *Phys. Rev. Lett.* **43**, 1726 (1979).